KERNFORSCHUNGSZENTRUM

KARLSRUHE

April 1963

KFK 180

Institut für Angewandte Kernphysik

Determination of Absolute Thermal Neutron Flux by Gold Foils

Wolfgang Pönitz

KERNREAKTOR
BAU- UND BETRIEBS-GESELLSCHAFT M.B.H.
KARLSRUHE

KERNFORSCHUNGSZENTRUM KARLSRUHE

April 1963 KFK 130

Institut für Angewandte Kernphysik

Determination of Absolute Thermal Neutron Flux by Gold Foils*

W. Pönitz

*) vorgetragen bei der Tagung der Euratom Reactor Dosimetry Working Group, Brüssel, 9. April 1963

Kernreaktor Bau- und Betriebsgesellschaft mbH
Karlsruhe

Determination of Absolute Thermal Neutron Flux by Gold Foils

by

W. Pönitz

Institut für Angewandte Kernphysik
Kernforschungszentrum Karlsruhe

1. Introduction

Because of its well-known activation cross section, gold is the most employed detector material for absolute thermal neutron flux measurements (1), (2).

More properties that make it important as a neutron detector are:

1. Gold has only one isotope.
2. Gold foils have good mechanical properties and are obtainable with high chemical purity.
3. The activation cross section is high (σ (0,0253 eV) = 98.8 ± 0.3 b (3)) and approximately proportional to 1/v in the thermal region.
4. Au^{198} has a simple decay scheme and an appropriate half-life.

Using the extension of the ß-γ coincidence method to the 4π ß-γ coincidence method (4) it is possible to determine the foil activity with high accuracy. On the other hand, using a 4π ß counter the equipment and the measurements are simple and low disintegration rates can be determined. Therefore, it is practical to use a 4π ß detector

and calibrate it by gold foils which were measured by the $4\pi\beta$-γ coincidence method.

This paper contains some general comments on absolute flux measurements with gold (section 2) and reports on the absolute counting method which is in use at Karlsruhe (section 3).

2. Activation in a Thermal Neutron Flux

2.1. Activation of Gold Foils

The activation rate, $C\ [cm^{-2}\ sec^{-1}]$, of a circular foil of thickness d, irradiated in a thermal neutron flux, $\phi_{th}(E)$, is

$$C = \phi_{th} \frac{\sqrt{\pi}}{2} \Sigma_{act}(E_T) \cdot d \cdot \left\{ G_0^{th} + G_1^{th} \right\}. \qquad (2.1)$$

$\Sigma_{act}(E_T)$ being the activation cross section at $E_T = kT$, and ϕ_{th} the absolute neutron flux. The function G_0^{th} includes the self shielding of the foil and the averaging over the Maxwell spectrum (5):

$$G_0^{th} = \frac{2}{\sqrt{\pi}\ \Sigma_{act}(E_T)} \int_0^\infty \Sigma_{act}(E)\ \frac{f_0(\Sigma_{tot} \cdot d)}{2\Sigma_{tot} \cdot d}\ \frac{E}{E_T} \cdot e^{-\frac{E}{E_T}} \cdot \frac{dE}{E_T} \qquad (2.2\ a)$$

$$f_0(\Sigma_{tot} d) = 1 - 2E_3(\Sigma_{tot} d). \qquad (2.2\ b)$$

Σ_{tot} is the total cross section and E_3 the third of the well-known Placzek-functions. For $d \to 0$, that is for the self shielding approaching zero, G_0^{th} becomes identical with the $g(E_T)$ factor given by WESTCOTT (6).

The factor G_1^{th} takes care of neutrons which have undergone a scattering collision within the foil and contribute to the activation afterwards. Assuming isotropic scattering, it is given by (7)

$$G_1^{th} = \frac{2}{\sqrt{\pi}\ \Sigma_{act}(E_T)} \cdot \int_0^\infty \frac{\Sigma_{act}(E)\ \Sigma_s(E)}{\Sigma_{tot}(E)}\ \frac{f_1(\Sigma_{tot} d)}{2\Sigma_{tot} d}\ \frac{E}{E_T} e^{-\frac{E}{E_T}} \cdot \frac{dE}{E_T} \qquad (2.3\ a)$$

$$f_1(\Sigma_{tot} d) = \int_0^d \left\{ E_2(\Sigma_{tot} x) + E_2(\Sigma_{tot}[d-x]) \right\} \qquad (2.3\ b)$$

$$\cdot \left\{ 1 - E_2(\Sigma_{tot} x) - E_2(\Sigma_{tot}[d-x]) \right\} \cdot 2_{1,1}\, dx$$

where Σ_s is the scattering cross section. G_o^{th} and G_1^{th} were averaged over the Maxwell spectrum (8); they are given in Tab. 1 and shown in Fig. 1.

2.2 Corrections Pertaining to the Flux Determination

The assumptions underlying equation (2.1) are only satisfied to a first approximation. Therefore, it is appropriate to give a discussion of the necessary corrections.

2.2.1 Activation by Epithermal Neutrons

It is possible to describe the neutron spectrum by two groups:

$$\Phi(E)dE = \Phi_{th} \cdot \frac{E}{E_T^2} e^{-\frac{E}{E_T}} \cdot \frac{dE}{E_T} + \Phi_{epi} \cdot \frac{\Delta(E)}{E} dE \qquad (2.4)$$

where Φ_{epi} is the epithermal flux per lethargy unit and $\Delta(E)$ a "joining function" (see for instance JOHANSSON et.al. (9)).

To eliminate the epithermal activation by a cadmium difference measurement, the difference ΔI between the resonance integral I_{epi} and the epicadmium resonance integral I_{Cd} must be considered. For activation one obtains

$$\begin{aligned} C_{epi} &= C_{Cd} + (C_{epi} - C_{Cd}) \\ &= \Phi_{epi} \cdot N \cdot \sigma_0 \cdot I_{Cd} + \Phi_{epi} \cdot N \sigma_0 \Delta I \\ C_{epi} &= C_{Cd} \left(1 + \frac{\Delta I}{I_{Cd}}\right). \end{aligned} \qquad (2.5)$$

N being the number of atoms per cm^3. I_{epi} and I_{Cd} were evaluated by BROSE (10). Tab. 1 gives the values and Fig. 2 shows $1 + \frac{\Delta I}{I_{Cd}}$ for gold foils at a cadmium thickness of 1 mm.

2.2.3 Perturbation of the Foil Activation

Eq. (2.1) is correct for a scattering medium with transport mean free path $\lambda_{tr} \to \infty$. For the real case with $\lambda_{tr} \neq \infty$ the activation is given by

$$C' = \frac{C}{1 + \chi_C} \,. \qquad (2.6)$$

χ_c is the foil depression factor and is proportional to the absorption by the foil

$$\chi_c = g\left(\frac{1}{2} - E_3(\Sigma_a d)\right). \tag{2.7}$$

Σ_a is the absorption cross section, g is given by SKYRME (11):

$$g = \frac{4}{\pi} \cdot \frac{R}{\lambda_{tr}} \cdot \left[1 - \frac{3\pi}{16}\frac{R}{L} + \frac{4}{15}\frac{R^2}{L^2} - \frac{\pi}{32}\frac{R^3}{L^3} + \cdots\right] \tag{2.8}$$

where L is the diffusion length and R is the radius of the circular foil.

2.2.3 Correction for the Finite Foil Radius

Eq. (2.1) was derived for an infinite foil. Taking account of the finite foil radius R, one obtains

$$C'' = C(1+\varepsilon). \tag{2.9}$$

ε was derived by HANNA (12)

$$\varepsilon = \frac{2\Sigma_{tot}\, d}{f_0(\Sigma_t, d)} \cdot \frac{d}{\pi R} \cdot \left(1 - \frac{\pi \Sigma_{tot}\, d}{6}\right). \tag{2.10}$$

2.2.4 Corrections for the Geometry of the Neutron Field

Eq. (2.1) holds for an isotropic flux. In a medium with grad $\Phi \neq 0$ eq. (2.1) is also correct if the activity is measured in a 4π geometry (7).

A further assumption for the derivation of eq. (2.1) is that the neutron flux is constant over the foil surface. If this is not the case, the activation rate is proportional to the average flux $\bar{\Phi} = \int \Phi(\vec{r})\, df / \int df$. To a first approximation, one has

$$\Phi(\vec{r}) = \Phi(\vec{r}_0) + (\vec{r} - \vec{r}_0)\left[\operatorname{grad} \Phi(\vec{r})\right]_{\vec{r}_0} \tag{2.11a}$$

$$\Phi(\vec{r}_0) = \bar{\Phi}(1-k), \quad k = \frac{1}{\pi R^2 \bar{\Phi}} \int (\vec{r} - \vec{r}_0)\left[\operatorname{grad} \Phi(\vec{r})\right]_{\vec{r}_0} df \tag{2.11b}$$

where $\emptyset\ (\vec{r}_o)$ is the neutron flux at $\vec{r}_o$, that is, at the centre of the foil.

3. Absolute Determination of the Au^{198} Activity

Various experiments with three different 4π ß proportional detectors showed that the counting rates for a gold foil differ only by 0,1 per cent. The long-time-stability of the detectors was checked using the Sr^{90} activity. It was found to be better than 0,1 per cent over a period of two years. Therefore, the 4π ß counter appeared to be a good instrument for standard measruements and it was decided to use it as a standard instrument.

The relationship between the 4π ß counting rate, $N_ß$, and absolute disintegration rate, N_o, is

$$N_ß = S_ß(d)\ N_o \qquad (3.1)$$

Eq. (3.1) defines the effictive ß-self absorption factor $S_ß(d)$. $S_ß(d)$ includes the ß-self absorption in the foil, the counting of internal conversion electrons in the ß-channel, decay scheme effects, γ-sensitivity of the ß-detector, bremsstrahlung effects, etc.

$S_ß(d)$ depends on the manner of the activation. For instance, there is a difference between $S_ß$ for thermal and epithermal activated foils (see fig. 3).

$S_ß(d)$ was determined by two methods which will be briefly described.

3.1 Determination of $S_ß(d)$ - First Method

The absolute disintegration rate, N_o, can be determined by the 4π ß-γ coincidence method (4). If $N_ß$ is the counting rate in the ß-channel, N_γ the counting rate in the γ-channel and N_c the coincidence counting rate, the following relation holds:

$$N_o = \frac{N_ß\ N_\gamma}{N_c} \cdot f(d). \qquad (3.2)$$

The function $f(d) = \prod_i h_i$ includes all corrections, h_i, which depend on the foil thickness (3). N_β, N_γ and N_c have to be corrected for background, dead-time and random coincidence.

For the first method to determine $S_\beta(d)$ gold foils of various thickness were irradiated and their activities were measured by the $4\pi\,\beta$-γ coincidence method. The absolute disintegration rates, N_o, were determined by eq. (3.2) with a calculated correction function f(d). Then $S_\beta(d)$ results from eq. (3.1).

The function f(d) in eq. (3.2) can be neglected on the following conditions:

1. The deexitations of the Hg^{198}-levels (see decay scheme Fig.3) occur only by γ-decay (do not occur through internal conversion).

2. The β- and γ-efficiencies are independent of the position in the detectors.

3. Isotropic emission of source and no angular correlation, if the probability to detect the β- or γ-decays differs from one.

4. The probability for detection of a β- or γ-ray is equal for a disintegration at any point in the source.

5. For each decay there results only one β, and at least one γ.

6. The β-detector counts only β's.

7. The γ-detector counts only γ's.

For gold foils these conditions are satisfied only in a first approximation. Therefore, the corresponding corrections must be discussed and evaluated.

3.1.1 Internal Conversion Electrons

For 4 per cent of the deexcitation of the first level of Hg^{198}, there results a conversion electron. Therefore, the ß-counting rate will be increased:

$$N_\beta = \{ \eta_\beta + (1 - \eta_\beta)\, \alpha' \eta_K \}\, N_0 \qquad (3.3a)$$

$$N_\gamma = \eta_\gamma (1 - \alpha')\, N_0 \qquad (3.3b)$$

$$N_C = \eta_\beta \eta_\gamma (1 - \alpha')\, N_0 . \qquad (3.3c)$$

Here, $\alpha' = (1 - \alpha)^{-1} \cdot \alpha$ where α is the total conversion coefficient. η_β is the probability to detect a ß decay in the ß-counter, η_γ is the probability to detect a γ decay in the γ-channel and η_K is the probability for detection of the conversion electron.

The energy of the K-conversion electrons is $\approx$ 330 keV, of the L-, M-, N-, ... conversion electrons $\approx$ 400 keV. From this difference in energy follows a difference in the probability to detect the conversion electrons, because of the ß-self absorption in the foil. Consequently, instead of eq. (3.3a) one must write:

$$N_\beta = \eta_\beta \left\{ 1 + \frac{1 - \eta_\beta}{\eta_\beta} \left(\alpha'_K \eta_{K_K} + \alpha'_{L,M} \eta_{K_{L,M}} \cdots \right) \right\} N_0 . \qquad (3.4)$$

With the equations (3.3) and (3.4) one obtains:

$$N_0 = \frac{N_\beta N_\gamma}{N_C} k_1 \; ; \; k_1 = 1 - \frac{1 - \eta_\beta}{\eta_\beta} \left(\alpha'_K \eta_{K_K} + \alpha'_{L,M} \eta_{K_{L,M}} \cdots \right) \qquad (3.5)$$

η_β was obtained from measured values $N_\gamma = \eta_\gamma N_0$ and $N_C = \eta_\beta \cdot \eta_\gamma \cdot N_0$

$\alpha_K = (2.95 \pm 0.15) \cdot 10^{-2}$ is the conversion coefficient of the K-level (13), (14), (15) and $\alpha_{L,M,\ldots} = 1.22 \cdot 10^{-2}$ is the coefficient for the further levels (14), (15). These values give $\alpha'_K = 2.36 \cdot 10^{-2}$ and $\alpha'_{L,M,\ldots} = 1.21 \cdot 10^{-2}$.

MEISTER (16) has evaluated the ß-self absorption for monoenergetic electrons by metallic indium foils. The agreement with the experiment is good. For gold the assumptions of MEISTER's theory are even better satisfied than in the case of indium. Therefore, η_{K_K} (d) and $\eta_{K_{L,M}}$ (d)

were evaluated here by this theory. The functions are shown in Fig. 4. The calculated h_1 are given in Tab. 2.

3.1.2 Detector Geometries and Angular Correlation

To be exact, one must average the ß- and γ-efficiencies over all points of the detectors and over all points in the source where decays occur (17). Taking the angular correlation into account, one obtains

$$N_\beta = \frac{1}{V_\beta}\cdot\frac{1}{V}\int\int N(\vec{r})\,\eta_\beta(\vec{r},\vec{r}')\,dV\,dV_\beta = N_0\cdot\overline{\eta_\beta}$$

$$N_\gamma = \frac{1}{V_\gamma}\cdot\frac{1}{V}\int\int N(\vec{r})\,\eta_\gamma(\vec{r},\vec{r}'')\,dV\,dV_\gamma'' = N_0\cdot\overline{\eta_\gamma} \qquad (3.6)$$

$$N_C = \frac{1}{V_\beta}\cdot\frac{1}{V_\gamma}\cdot\frac{1}{V}\int\int\int N(\vec{r})\,w(\vec{r}',\vec{r}'')\,\eta_\beta(\vec{r},\vec{r}')\,\eta_\gamma(\vec{r},\vec{r}'')\,dV\,dV_\beta\,dV_\gamma'' = N_0\cdot\overline{\eta_\beta\,\eta_\gamma}$$

V_β and V_γ are the volume of the ß- and γ-detectors, respectively. V is the volume of the source. $\eta_\beta(\vec{r},\vec{r}')$ and $\eta_\gamma(\vec{r},\vec{r}'')$ are the probabilities for detection of a decay at $\vec{r}$ in the source by the ß- or γ-detector at $\vec{r}'$ or $\vec{r}''$, respectively. $N(\vec{r})$ is the disintegration rate at $\vec{r}$ and $w(\vec{r}',\vec{r}'')$ is the angular correlation. The correction, h_2, which is given by

$$N_0 = \frac{N_\beta N_\gamma}{N_C}\cdot h_2\,; \qquad h_2 = \frac{\overline{\eta_\beta\,\eta_\gamma}}{\overline{\eta_\beta}\;\overline{\eta_\gamma}} \qquad (3.7)$$

was calculated (8) for the extreme case of a rectilinear path for ß-rays in the foil. h_2 and the correlating geometry is shown in Fig.5.

3.1.3 Correction for Complex Decay Scheme

Fig. 3 shows the decay scheme of Au^{198}. The direct ß-decay of Au^{198} to the ground state of Hg^{198} can be neglected. Because of the difference of γ-sensitivities of the three γ-energies, the equations for the coincidence method must be expanded (4):

$$\begin{aligned} N_\beta &= (a\,\eta_{\beta a} + b\,\eta_{\beta b})\,N_0 \\ N_\gamma &= (a\,\eta_{\gamma a} + b\,\eta_{\gamma b})\,N_0 \\ N_C &= (a\,\eta_{\beta a}\,\eta_{\gamma a} + b\,\eta_{\beta b}\,\eta_{\gamma b})\,N_0 . \end{aligned} \qquad (3.8)$$

a = 0.99 and b = 0.01 (see Fig. 3). In these experiments the 412 keV-γ-line was used. Therefore, it is possible to write $\eta_{\gamma a} = \eta_\gamma$ and $\eta_{\gamma b}$ 0.32 η_γ. The factor 0.32 results from the branching ratio for deexcitation of the second level of Hg^{198} (18). The resulting expression is

$$N_0 = \frac{N_\beta N_\gamma}{N_c}\, k_3\,,\quad k_3 = 1 + 0.0017\,\frac{\eta_{\beta a} - \eta_{\beta b}}{\eta_{\beta a} + 0.1\,\eta_{\beta b}} \approx 1 + 0.0017 \cdot \left(1 - \frac{\eta_{\beta b}}{\eta_{\beta a}}\right). \qquad (3.9)$$

$\eta_{\beta a}$ and $\eta_{\beta b}$ are calculated from (19):

$$\eta_\beta = \frac{1 - e^{-\alpha d}}{\alpha d}\,. \qquad (3.10)$$

The ß-absorption coefficient, α, as given by MEISTER (20) and GLEASON (21), is

$$\alpha = 17.0\,\rho \cdot E_{\beta max}^{-1.43} \cdot \left(\frac{Z}{13}\right)^{0.215}\,. \qquad (3.11)$$

One obtains for gold

$$\alpha = 457 \cdot E_{\beta max}^{1.43} \qquad (3.12)$$

Evaluated values of h_3 are given in Tab. 2.

3.1.4 γ-Sensitivity of the ß-Detector

The γ-quanta can produce counts in the ß-detector (e.g. by photoelectric effect on the wall of the ß-detector). The necessary correction is given by CAMPION (4):

$$N_\beta = \{\eta_\beta + (1 - \eta_\beta)(\eta_\beta)_\gamma\}\, N_0$$

$$N_\gamma = \eta_\gamma\, N_0 \qquad (3.13)$$

$$N_c = \{\eta_\beta \eta_\gamma + (1 - \eta_\beta)\,\eta_c\}\, N_0\,.$$

$(\eta_\beta)_\gamma$ is the probability for detecting a γ-quantum in the ß-counter, η_c is the probability that a coincidence occurs when the ß is not counted. Interpolating CAMPION's ($(\eta_\beta)_\gamma - \frac{\eta_c}{\eta_\gamma}$)-curves, one obtains:

$$N_0 = \frac{N_\beta N_\gamma}{N_c} \cdot k_4\,;\quad k_4 = 1 - 0.0035\,\frac{1 - \eta_\beta}{\eta_\beta}\,. \qquad (3.14)$$

For values of h_4, see Tab. 3.

3.1.5 Electrons from Photoelectric Effect and Compton Scattering

The monoenergetic electrons from the photoelectric effect in the foil can be counted by the 4π ß-detector, if the associated ß-particle is not registered. The counting rate of the ß-detector is

$$N_\beta = \left\{ \eta_\beta + (1-\eta_\beta)\left(1 - \frac{f_0(\sigma d)}{2\sigma d}\right) \frac{\sigma_{ph}}{\sigma} \left(a\,\eta_{K_{II}} + b\,\eta_{L,M\ldots}\right) \right\} N_0 \quad (3.15)$$

σ is the total linear attenuation coefficient and σ_{ph} is the linear attenuation coefficient for the photoelectric effect. $1 - \frac{f_0(\sigma d)}{2\sigma d}$ is the probability that γ-interaction has taken place. a and b are the relative occurances of photoelectric effects at the K-level or L-, M-, ... levels, respectively, At the same time, by the Compton effect, one obtains:

$$N_\beta = \left\{ \eta_\beta + (1-\eta_\beta)\left(1 - \frac{f_0(\sigma d)}{2\sigma d}\right) \frac{\sigma_{co}}{\sigma} \eta_{co} \right\} N_0 \quad (3.16)$$

where η_{co} is the probability for counting the Compton electron in the ß-detector and σ_{co} is the linear attenuation coefficient for the Compton effect.

If the energy loss of the γ-quantum is smaller than the "half window energy width", ΔE, of the differential discriminator, the coincidences which can occur are given by

$$N_C = \left\{ \eta_\beta \eta_\gamma + (1-\eta_\beta)\eta_\gamma \left(1 - \frac{f_0(\sigma d)}{2\sigma d}\right) \frac{\sigma_{co}}{\sigma} n(\Delta E) \eta'_{co} \right\} N_0 . \quad (3.17)$$

$n(\Delta E)$ is the relative occurance of the Compton effect with the energy loss 0 ... $\Delta E/2$. η'_{co} is the probability of detecting these Compton electrons. From the equations (3.13), (3.14) and (3.15) follows:

$$N_0 = \frac{N_\beta N_\gamma}{N_C} \cdot h_5 \; ; \; h_5 = 1 - \frac{1-\eta_\beta}{\eta_\beta}\left(1 - \frac{f_1(\sigma d)}{2\sigma d}\right) \left\{ \frac{\sigma_{ph}}{\sigma}\left(a\,\eta_{K_{II}} + b\,\eta_{L,M\ldots}\right) + \frac{\sigma_{co}}{\sigma}\left(\eta_{co} - n(\Delta E)\eta'_{co}\right) \right\} . \quad (3.18)$$

σ_{ph} = 2.45 cm^{-1} and σ_{co} = 1.43 cm^{-1} are given by DAVISSON and EVANS (22). a = o.35 and b= o.15 (23). n (Δ E) was evaluated from energy spectra of Compton electrons (24).

It would have been possible to calculate the self absorption factors η_{co} and η'_{co} of Compton electrons with well-known energy spectra by MEISTER's theory (16). However, because of the extensive calculations involved with this theory, η_{co} and η'_{co} were determined by eq. (3.11). The error was assumed to be 20 per cent. Values of h_5 are given in Tab.2.

3.1.6 Bremsstrahlung

The most frequent ß-energy of 0.959 MeV is higher than the 0.412 MeV-γ-peak. Therefore, it is possible to count bremsstrahlung quanta in the γ-channel. The bremsstrahlung quantum and the ß can produce a coincidence if the γ is not counted. The equations are

$$\begin{aligned} N_\beta &= \eta_\beta N_0 \\ N_\gamma &= \left\{ \eta_\gamma + (1-\eta_\gamma)\,\eta_{Br}\,\frac{N_{Br}(\Delta E)}{N_0} \right\} N_0 \\ N_C &= \left\{ \eta_\beta \eta_\gamma + (1-\eta_\gamma)\,\eta_{Br}\,\eta'_\beta \cdot \frac{N_{Br}(\Delta E)}{N_0} \right\} N_0 . \end{aligned} \tag{3.19}$$

$\eta_{Br} \approx \eta_\gamma$ is the probability for detecting the bremsstrahlung quanta $N_{Br}(\Delta E)$ of energy $E_\gamma \pm \frac{\Delta E}{2}$. η'_β is the probability for detecting the ß-particles which have caused a bremsstrahlung quantum with the same energy. The correction, h_6, becomes

$$N_0 = \frac{N_\beta N_\gamma}{N_C} h_6 , \qquad h_6 = 1 + (1-\eta_\gamma)\,\frac{N_{Br}(\Delta E)}{N_0}\left(\frac{\eta'_\beta}{\eta_\beta} - 1\right) \tag{3.2o}$$

Monoenergetic electrons of energy E' produce in a thick target bremsstrahlung of energy E (24):

$$d n_{Br} = N_0 \cdot i\, k\, Z \cdot \frac{E'-E}{E}\, dE . \tag{3.21}$$

k = 7 · 10^{-4} MeV^{-1}, Z is the atomic number. The average value, over the ß-energy spectra, is:

$$\frac{1}{N_0}\,\frac{d n_{Br}}{dE} = i\, k\, Z \cdot \frac{\int_E^{E_{max}} \frac{E'-E}{E} f(E')\, dE'}{\int_E^{E_{max}} f(E')\, dE'} = w(E) . \tag{3.22}$$

A further integration over the window energy width of the differential discriminator gives

$$\frac{n_{\beta r}(\Delta E)}{N_0} = \int_{E_r - \frac{\Delta E}{2}}^{E_r + \frac{\Delta E}{2}} m(E)\, dE. \qquad (3.23a)$$

For a thick target, the absorption factor is 1. Therefore, for a "self absorption target" one obtains

$$\frac{N_{\beta r}(\Delta E)}{N_0} = (1 - \eta_\beta)\, \frac{n_{\beta r}(\Delta E)}{N_0} \qquad (3.23b)$$

where $1 - \eta_\beta$ is the absorption probability. The equation (3.22) and (3.23a) were evaluated graphically. One obtains $\frac{n_{\beta r}}{N_0} = 0.008$ for $\Delta E/E_\gamma = 0.1$. η'_β was calculated by eq. (3.11) with a maximum energy $E_{\beta max} - E_\gamma \approx 0.55$ MeV. Values of h_6 are given in Tab. 2.

3.1.7 Determination of $S_\beta(d)$

The function $f(d) = \prod_{i=1}^{6} h_i$ is shown in Fig. 6.

The measured values N_β and $\frac{N_\beta N_\gamma}{N_C}$, used to determine $S_\beta(d)$ for thermal and for epithermal irradiated gold foils, are given in Tab. 3. Fig. 7 shows $S_\beta^{th}(d)$ and Fig. 8 $S_\beta^{epi}/S_\beta^{th}$ as functions of foil thickness d.

3.2 Determination of $S_\beta(d)$ - Second Method

The activity, N_0, of a foil of thickness d and surface F, irradiated in a thermal flux Ø, is (see the equations (3.1) and 3.2) in section 2):

$$N_0 = \phi_{th} \frac{\sqrt{\pi}}{2} \Sigma_{act}(E_T)\, d \cdot F \left\{ G_0^{th} + G_1^{th} \right\} \frac{1+\varepsilon}{1+x_c} \qquad (3.24)$$

$$= \frac{N_p N_\gamma}{N_C} \cdot f(d) = \frac{N_\beta}{S_\beta(d)}.$$

In these equations, for d → 0, the factors

$\{G_0^{th} + G_1^{th}\}$	approach	g (E_T)
$1+\varepsilon$	"	1
$1+x_c$	"	1
$f(d)$	"	1
$S_\beta(d)$	"	1.

Furthermore, N_β, N_γ, N_c and N_o approach zero causing the corrections for random coincidences and dead-time to approach zero.

Therefore, foils of various thicknesses were irradiated in the same neutron flux and counted with the 4π ß-γ coincidence equipment. In each case, $\frac{N_\beta N_\gamma}{N_c \cdot W}$ (with W = weight of the foil) was formed and the resulting figures plotted against W. Extrapolation to $W \rightarrow 0$ yields

$$\left(\frac{N_\beta N_\gamma}{N_c W}\right)_{d=0} = a = \Phi_{th} \frac{\pi}{2} \frac{\Sigma_{act}(E_T)}{\beta} \cdot g(E_T) \cdot \qquad (3.25)$$

Using this result, eq. (3.24) becomes

$$S_\beta(d) = \frac{g(E_T)}{a\left(G_o^{th} + G_1^{th}\right)} \cdot \frac{1+\chi_c}{1+\varepsilon} \cdot \frac{N_\beta}{W} \qquad (3.26)$$

and permits immediately the calculation of $S_\beta(d)$ since g (E_T), $\left\{G_o^{th} + G_1^{th}\right\}$, $1 + \varepsilon$ and $1 + \chi_c$ can be calculated by the methods outlined in section 2. The values of $S_\beta^{th}(d)$ thus obtained are given in Tab. 4 and shown in Fig. 7. One sees in this figure that the agreement of $S_\beta^{th}(d)$ with the $S_\beta^{th}(d)$ from the first method is very good.

With these $S_\beta^{th}(d)$-values it is possible to determine the Au^{198}-activities of gold foils by 4π ß-detector measurements with an accuracy of 0.2 - 0.3 %. Therefore, it should be possible to determine the absolute thermal neutron flux with an accuracy of 0.5 per cent.

(1) I.F. Raffle; J. Nucl. Energy, Part A, 10, 8 (1958)

(2) E.R. Mosburg, W.M. Murphey; Reactor Science and Technology, Parts A/B; 14, 25 (1961)

(3) F. Gould et al.; Bull. Am. Phys. Soc., II, 2, 42 (1957)

(4) P.J. Campion; International Journal of Applied Radiation and Isotopes, 4, 232 (1953)

(5) K.H. Beckurts et al.; to be published in Nucl. Science and Eng.

(6) C.H. Westcott, EANDC (Can)-4

(7) H. Meister, Zeitschrift für Naturforschung, 13 a, 722, (1953)

(8) W. Pönitz, Diplomarbeit Karlsruhe 1962

(9) E. Johansson et al.; J. Nucl. Energy, A, 11, 101 (1960)

(10) M. Brose, Dissertation Karlsruhe 1962

(11) T.H.R. Skyrme, "Reduction in Neutron Density Caused by an Absorbing Disc" MS-91

(12) G.C. Hanna; Nucl. Science and Eng., 15, 325 (1963)

(13) B.G. Pettersson u.a., Nuclear Physics, 24, 243 (1961)

(14) Nuclear Data Sheets, National Academy of Science

(15) W. Kunz et.al.; Tabellen der Atomkerne, Teil 1, Band 2 (1960)

(16) H. Meister; Zeitschrift f. Naturforschung, 13 a, 809 (1958)

(17) J.L. Putman; A.E.R.E. Report I/M 26 (1953)

(18) D. Strominger et al.; Rev. of Mod. Phys., 30, 585 (1958)

(19) K. Wirtz and K.H. Beckurts; Elementare Neutronenphysik, Springer 1958

(20) H. Meister; Dissertation, Göttingen 1957, see (7)

(21) G.J. Gleason; Nucleonics, 8, 12 (1951)

(22) Ch.M. Davisson and R.D. Evans; Rev. of Mod. Phys., 24, 2 (1952)

(23) K. Siegbahn; Beta- and Gamma-Ray Spectroscopy, North-Holland Publishing Company Amsterdam, 1955

(24) R.D. Evans; The Atomic Nucleus, McGraw-Hill Book Comp., Inc. 1955

Table 1: G_o^{th} (Σ_{tot} d; 0.0253 eV); G_1^{th} (Σ_{tot} d; 0.0253 eV) and $1 + \frac{\Delta I}{I_{Cd}}$

d / μ *)	G_o^{th}	G_1^{th}	$1 + \frac{\Delta I}{I_{Cd}}$
0	1.005199	0.000000	1.0459
1	1.002156	0.000173	1.0492
2	0.999823	0.000317	1.0531
4	0.995644	0.000576	1.0602
6	0.991855	0.000813	1.0661
8	0.988281	0.001035	1.0725
10	0.984870	0.001245	1.0780
20	0.969500	0.002156	1.1007
40	0.943795	0.003826	1.1323
60	0.921590	0.004859	1.1561
80	0.901632	0.005920	1.1749
100	0.883380	0.006985	1.1907
200	0.808044	0.010327	1.2469

*) d were evaluated by ρ = 19.32 g/cm^3

Table 2: Corrections for determination of the gold foils activities by the 4π ß-y coincidence method

d/u	h_1	h_2	h_3	h_4	h_5	h_6	f (d)	$\frac{\Delta f}{f}$ in %
0.517	0.9989	1.0003	1.0001	0.9999	1.0000	0.9998	0.9989	0.05
1.035	0.9976	1.0008	1.0002	0.9998	0.9999	0.9996	0.9979	0.07
2.588	0.9955	1.0017	1.0005	0.9996	0.9996	0.9993	0.9972	0.1
3.623	0.9948	1.0018	1.0006	0.9995	0.9995	0.9992	0.9953	0.1
5.176	0.9925	1.0019	1.0008	0.9994	0.9990	0.9990	0.9924	0.2
7.764	0.9899	1.0020	1.0010	0.9991	0.9981	0.9987	0.9887	0.2
10.352	0.9872	1.0021	1.0012	0.9989	0.9970	0.9985	0.9848	0.3
15.528	0.9833	1.0022	1.0013	0.9984	0.9946	0.9980	0.9778	0.3
20.703	0.9805	1.0024	1.0014	0.9979	0.9922	0.9978	0.9723	0.4
25.879	0.9790	1.0025	1.0015	0.9974	0.9903	0.9974	0.9683	0.5
36.231	0.9771	1.0027	1.0016	0.9963	0.9862	0.9968	0.9609	0.6
46.583	0.9756	1.0028	1.0016	0.9950	0.9821	0.9964	0.9541	0.7
56.935	0.9745	1.0030	1.0017	0.9935	0.9812	0.9961	0.9516	0.8

Table 3: ß-self absorption for thermal and epithermal irradiated gold foils

d/µ	$N_ß$	$\frac{N_ß N_\gamma}{N_c}$	f(d)	$S_ß^{th}(d)$	$\frac{\Delta s}{s}$ in %
3.35	16.446	18.735	0.9966	0.8808	0.2
5.27	13.497	16.142	0.9924	0.8425	0.3
5.42	25.242	30.307	0.9920	0.8396	0.3
5.70	10.587	12.783	0.9916	0.8352	0.3
9.49	22.655	29.532	0.9861	0.7779	0.4
10.50	13.624	18.274	0.9845	0.7573	0.4
11.01	22.450	30.372	0.9842	0.7510	0.4
20.04	14.434	23.333	0.9737	0.6353	0.5
21.87	16.376	27.483	0.9716	0.6133	0.5
24.50	14.637	25.705	0.9694	0.5874	0.6
26.94	16.377	38.043	0.9673	0.5634	0.6
32.03	74.002	149.070	0.9636	0.5152	0.7
50.53	17.436	47.608	0.9536	0.3841	0.8
52.78	24.337	68.775	0.9525	0.3715	0.8
				$S_ß^{epi}(d)$	
5.43	10.932	13.103	0.9920	0.841	0.4
16.71	54.135	81.140	0.9768	0.683	0.4
23.26	36.705	61.497	0.9705	0.615	0.5
32.14	41.509	78.131	0.9637	0.538	0.7
52.12	30.651	77.687	0.9530	0.414	0.8

Table 4: Determination of the S_{β}^{th} (d) by the extrapolation method

d/u	N_{β}/min	$\frac{N_{\beta}}{W}$ min/mg	$G_o^{th}+G_1^{th}$	$\frac{1+\chi_c}{1+\bar{c}}$	S_{β}^{th}(d)	$\frac{\Delta s}{s}$ in %
2.99	14 698.7	1003.3	0.997	1.0006	0.879	0.3
4.91	23 219.6	961.1	0.991	1.0010	0.848	0.3
11.03	45 662.9	841.9	0.984	1.0024	0.749	0.3
11.04	45 648.3	840.8	0.984	1.0024	0.748	0.3
31.97	88 315.1	561.8	0.955	1.0065	0.5170	0.3
32.02	87 665.4	556.9	0.955	1.0065	0.5134	0.3
52.13	101846.6	397.3	0.934	1.0073	0.3740	0.3
52.15	101 430.5	395.6	0.934	1.0073	0.3723	0.3
98.29	106 521.8	220.4	0.889	1.0108	0.2184	0.3
100.15	106 418.5	216.1	0.890	1.0109	0.2139	0.3

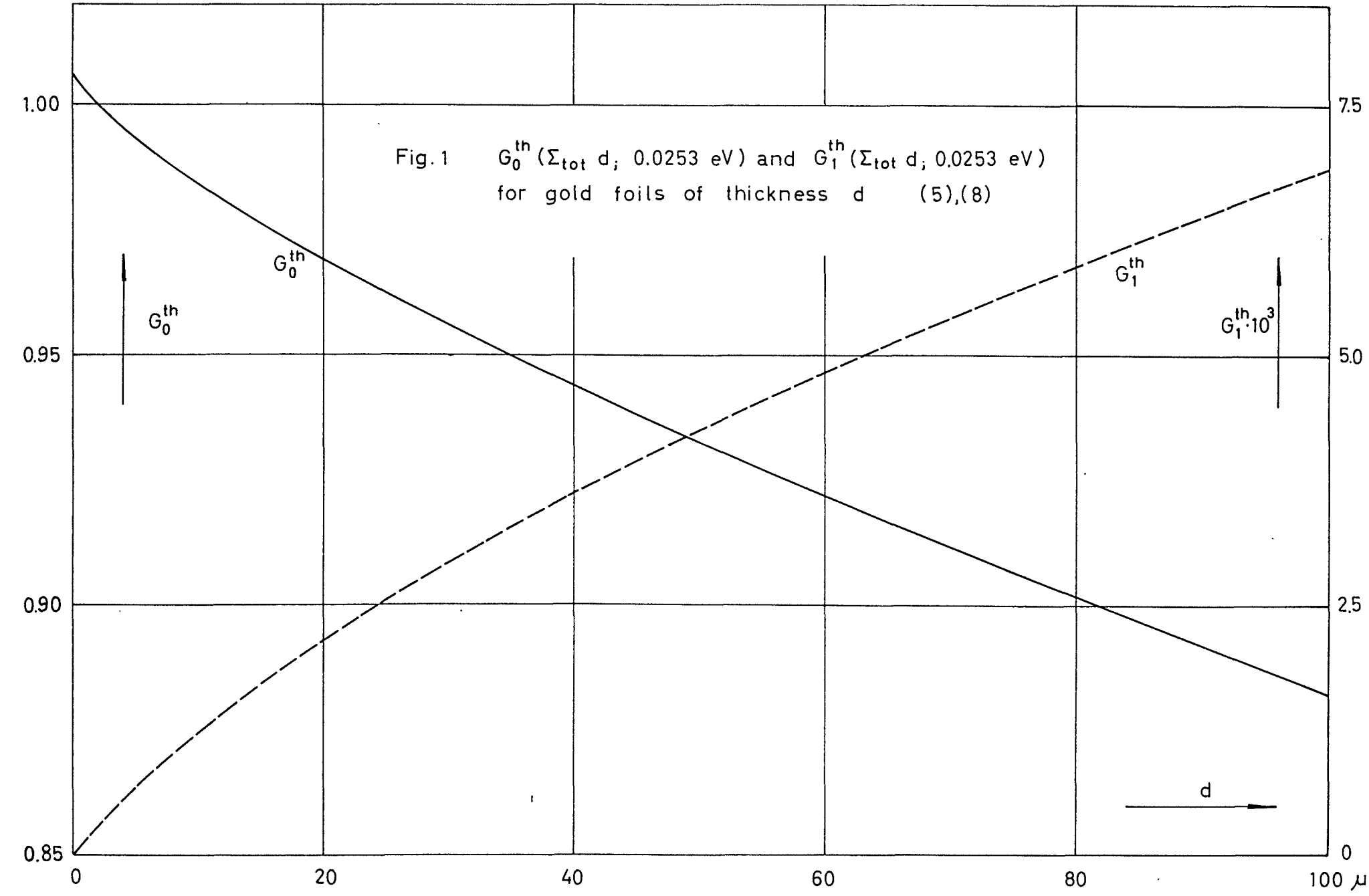

Fig. 1 $G_0^{th}(\Sigma_{tot}\, d;\ 0.0253\ eV)$ and $G_1^{th}(\Sigma_{tot}\, d;\ 0.0253\ eV)$ for gold foils of thickness d (5),(8)

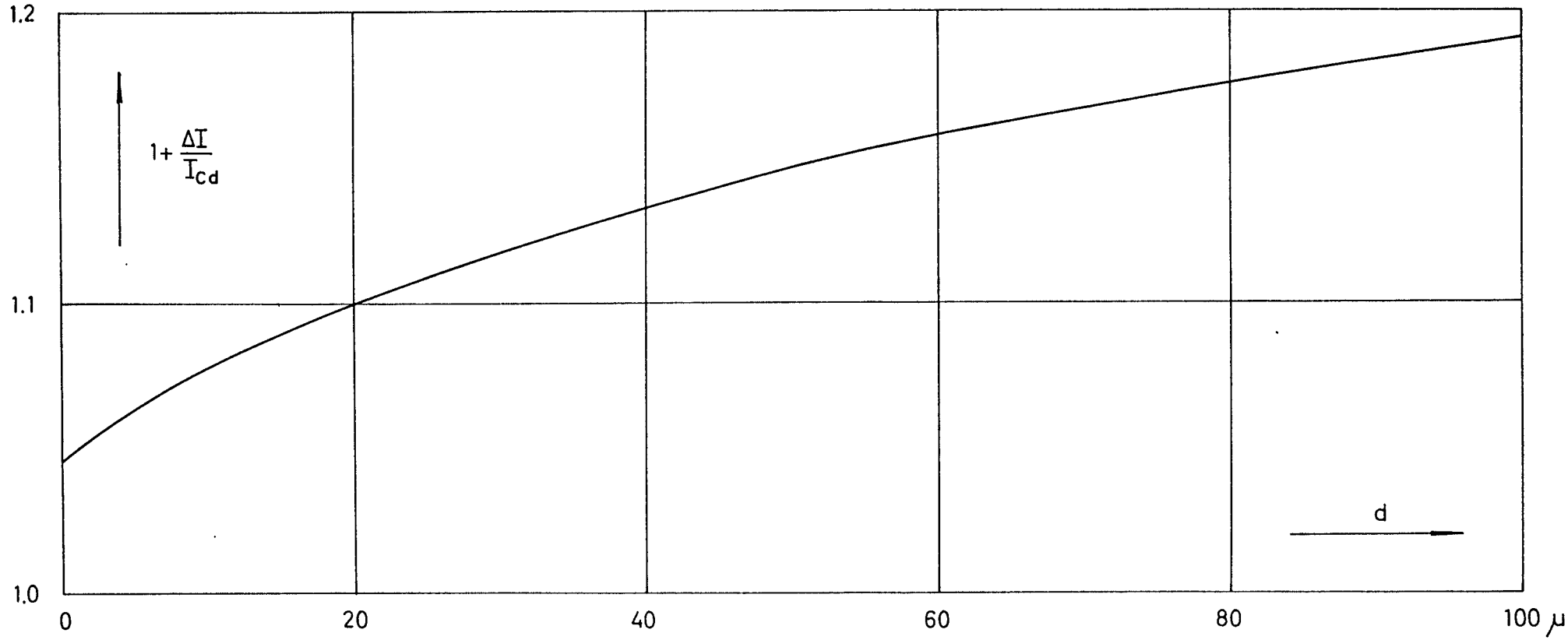

Fig. 2 $1+\frac{\Delta I}{I_{Cd}}$ for gold foils under 1 mm Cd (10)

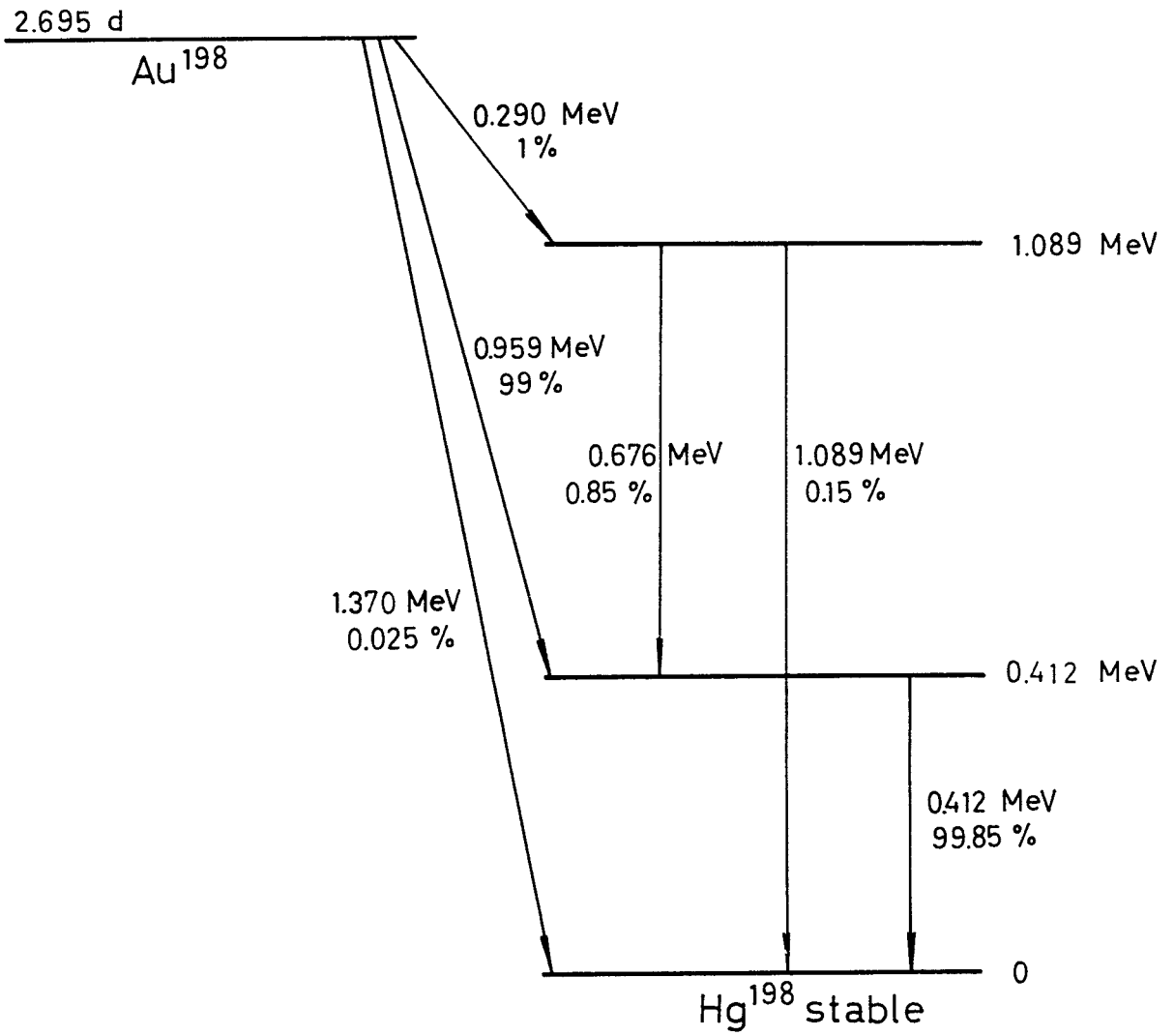

Fig. 3 Decay scheme of Au^{198}

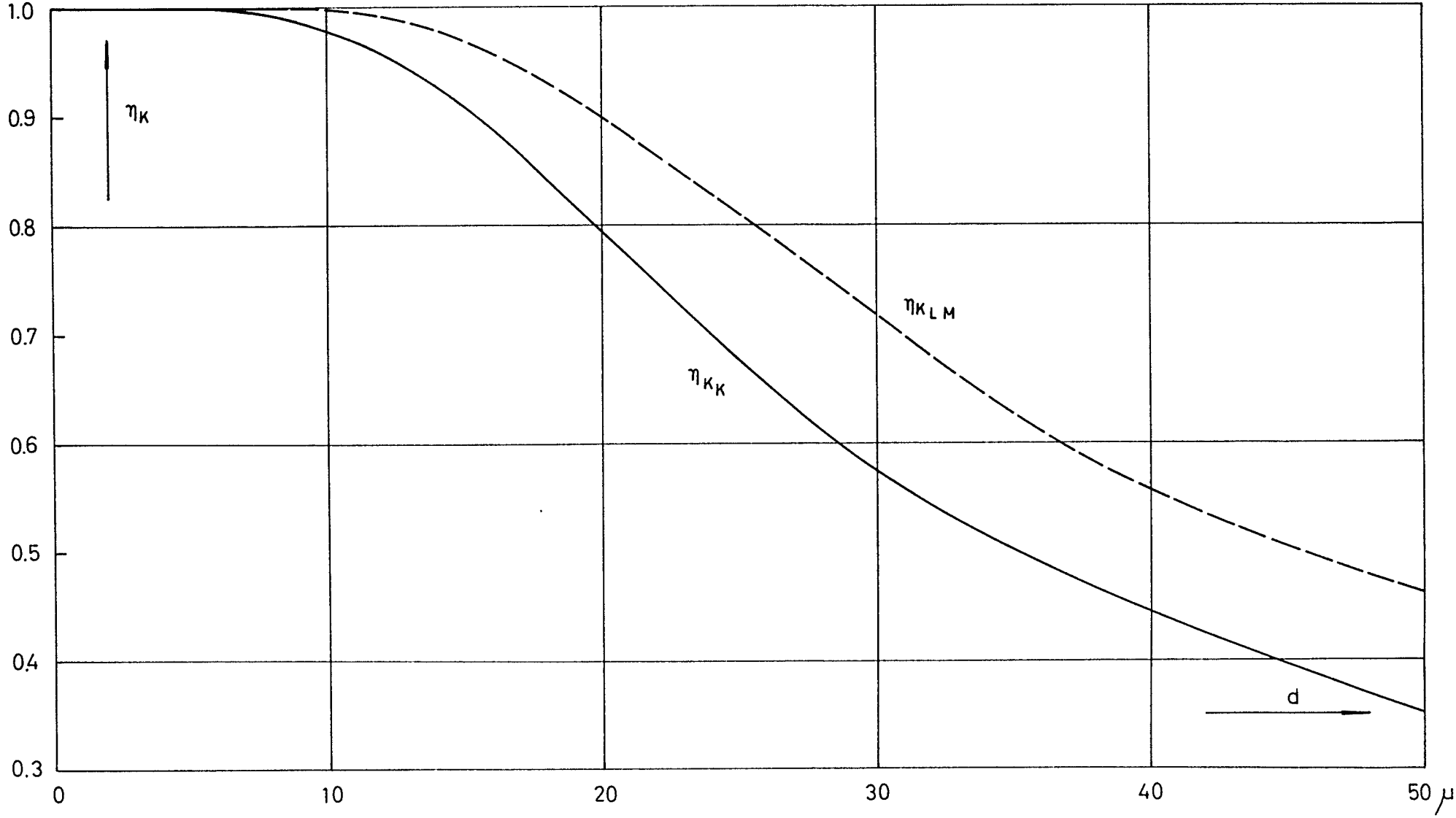

Fig. 4 Self absorption for monoenergetic electrons for gold foils

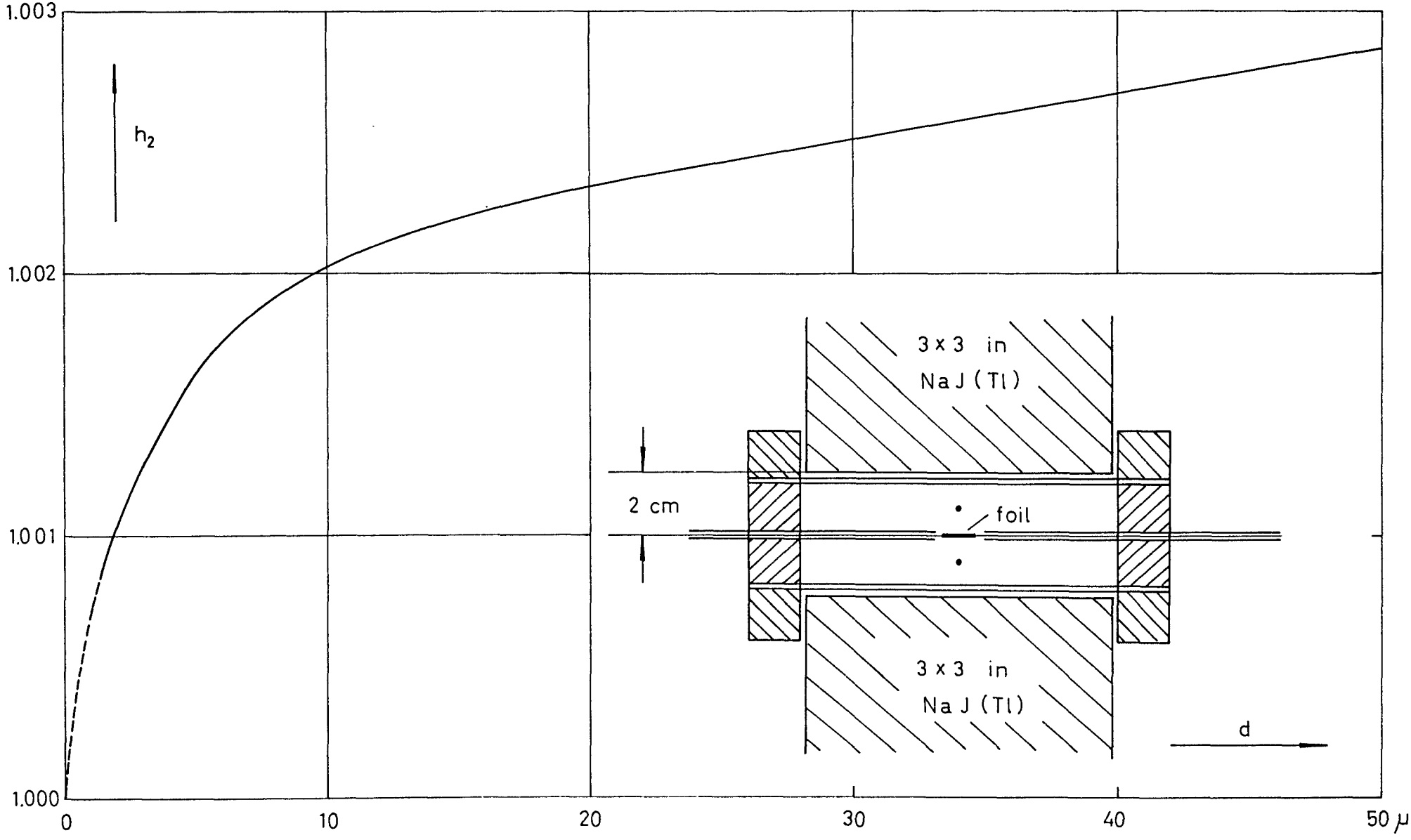

Fig. 5 Correction h_2 for detector geometry and angular correlation

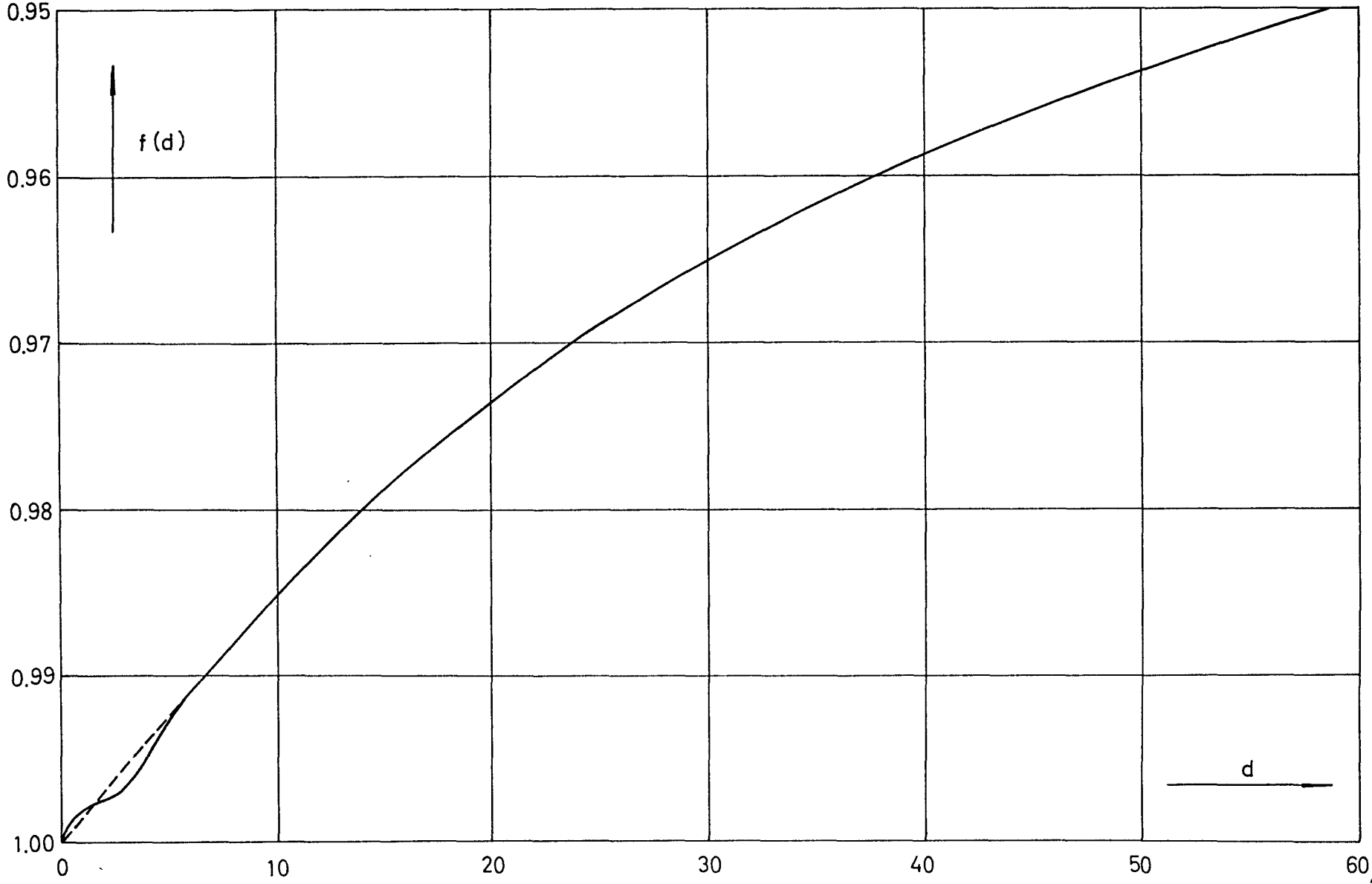

Fig. 6 Total correction f (d)

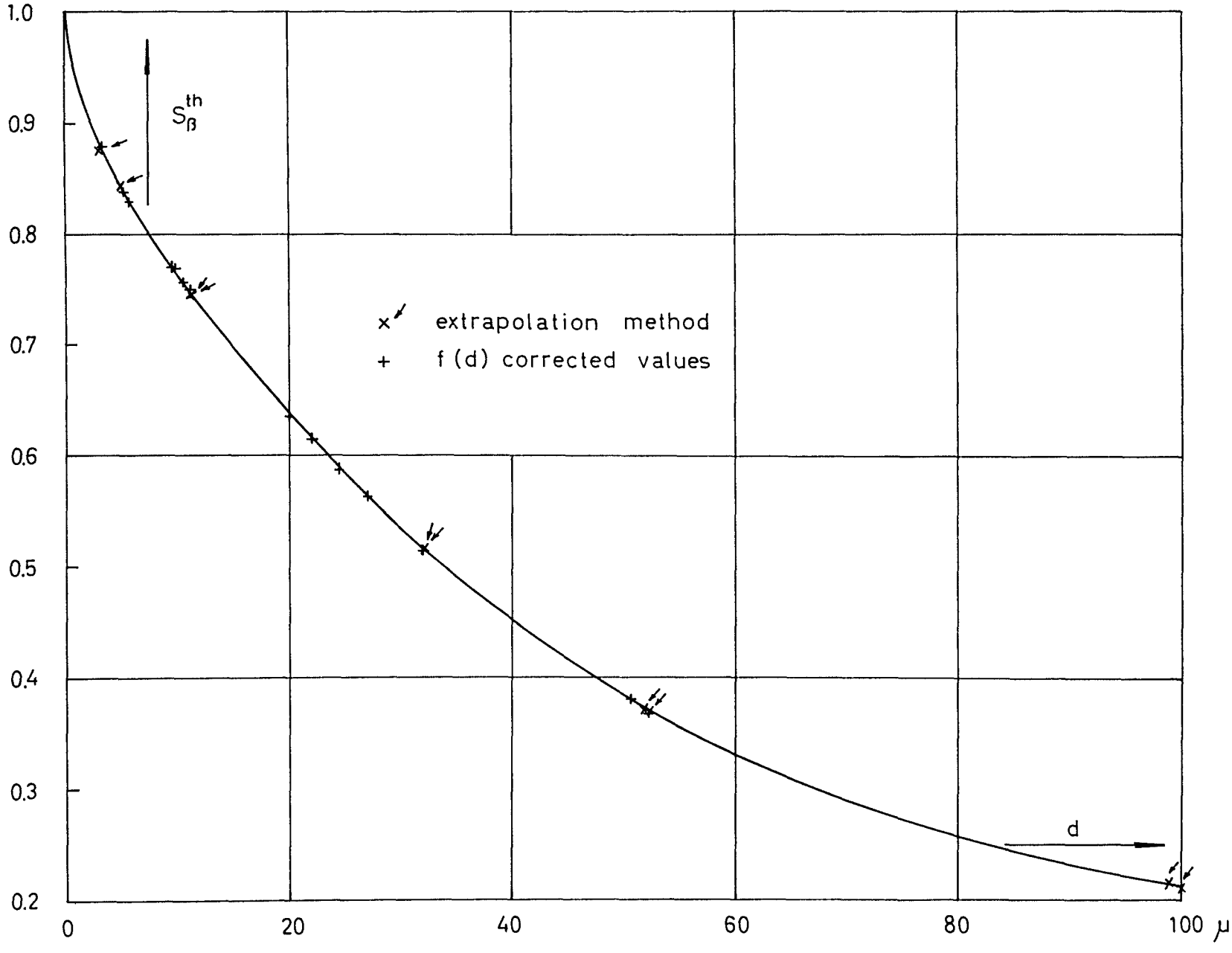

Fig. 7 β-self absorption $S_\beta^{th}(d)$ for thermal activated gold foils

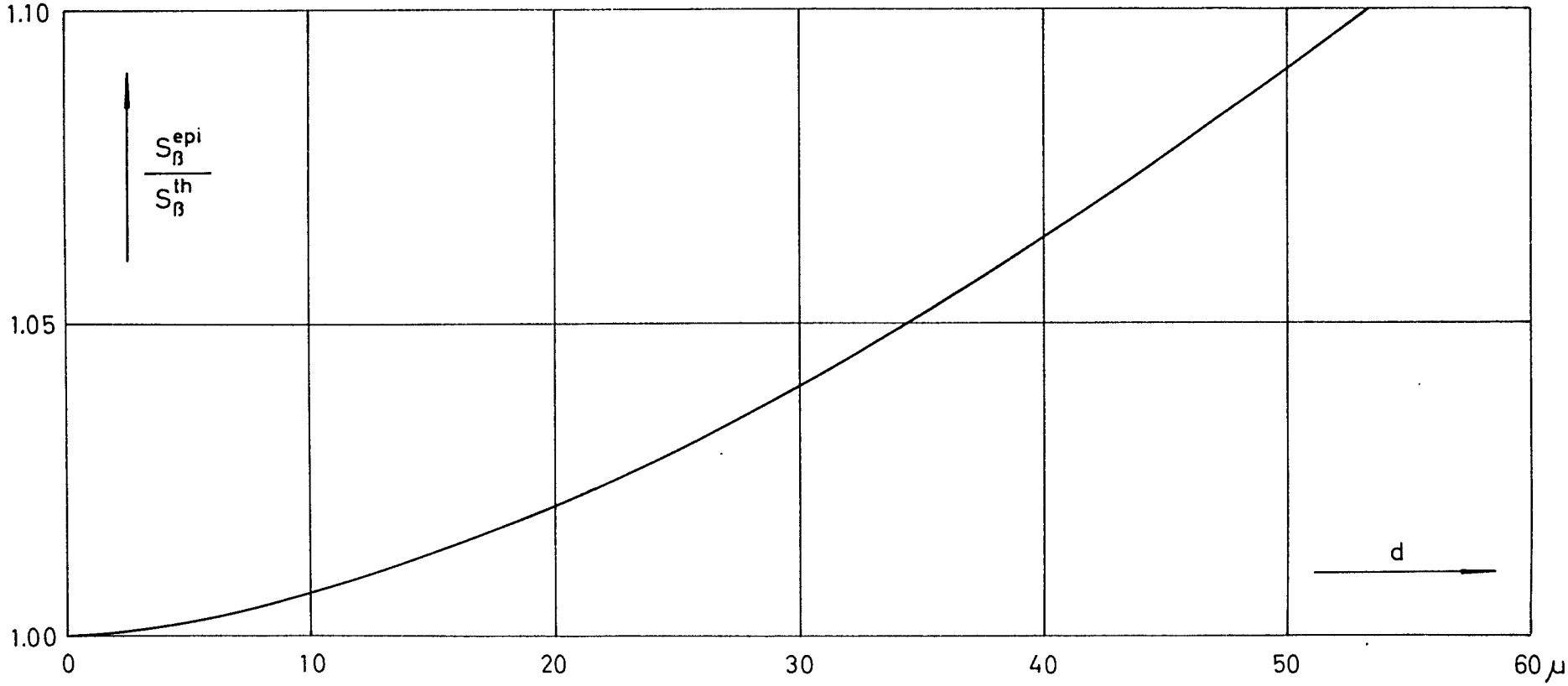

Fig. 8 $\frac{S_\beta^{epi}}{S_\beta^{th}}$ for gold foils

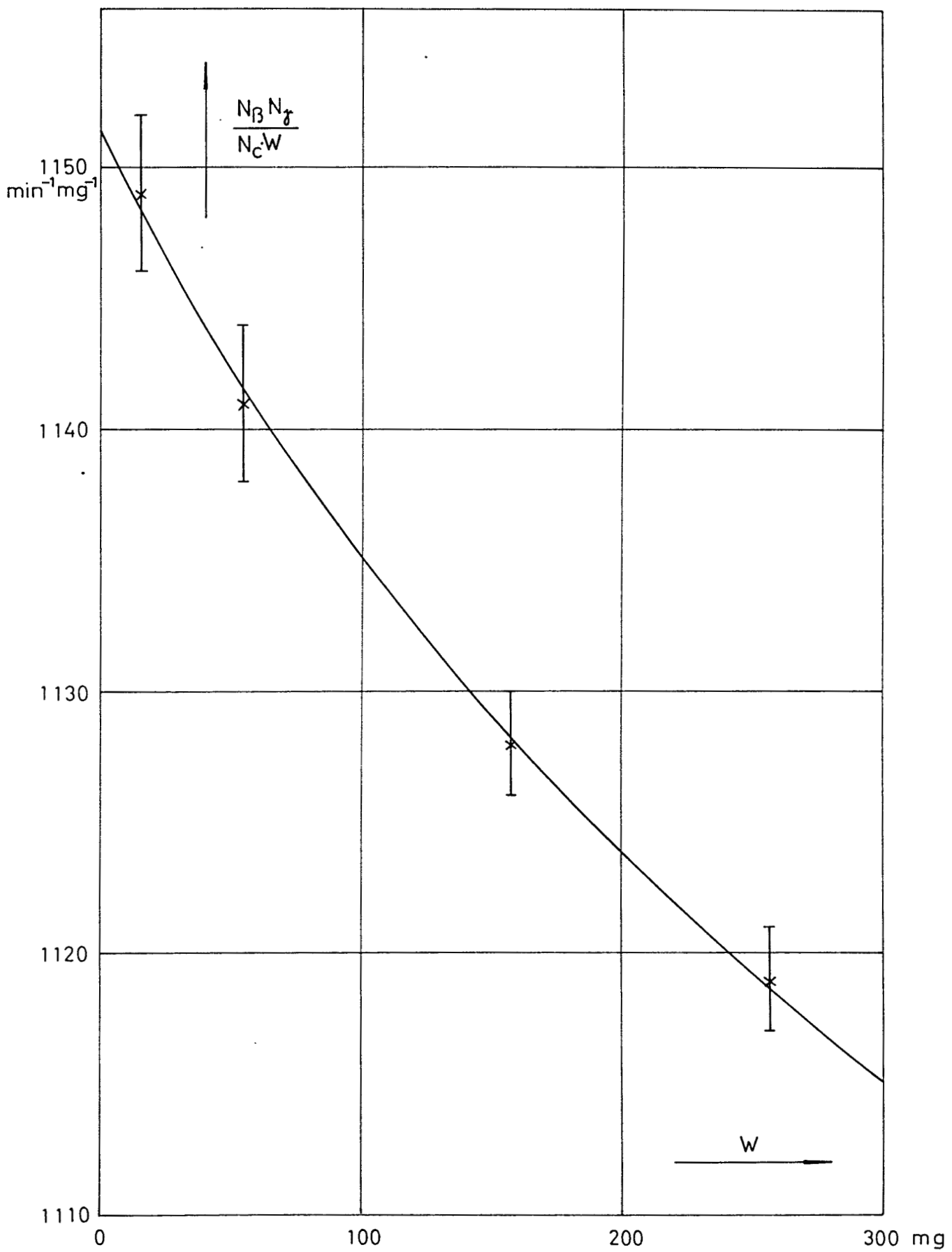

Fig. 9 Extrapolation of $\frac{N_\beta N_\gamma}{N_c \cdot W}$ for a resolving power of 10 %